JOURNAL GEOLOGICAL SOCIETY OF INDIA
Vol.86, August 2015, pp.223-232

# Zircon U–Pb Age and Geochemical Characteristics of Ore-bearing Granodiorite Porphyry in the Duobuza Porphyry Copper Deposit, Tibet

Guangchun Fei[1,2], Xiong-Zhou[3*], Ji-Duo[4], Yu-Zhou [2,3], Chun-Qi Wen[2], Quan-Wen[2], Yangyang He[2], Yan Huo[2], Zhengxi Yang[2], Jinshu Zhang[4], Hongfei Liu[4]

[1]Key Laboratory of Tectonic Controls on Mineralization and Hydrocarbon Accumulation, Ministry of Land and Resources, Chengdu University of Technology, Chengdu, 610059, China

[2]College of Earth Sciences, Chengdu University of Technology, Chengdu, 610059, Sichuan,China

[3]Institute of Multipurpose Utilization of Mineral Resources, Chinese Academy of Geological Sciences, Chengdu, 610041,China

[4]Geological and Mineral Resources Exploration Bureau of Tibet, Lasa, Tibet, China

*Email: fgc73177317@sina.com, zhouxiong27@163.com

**Abstract:** The Duobuza deposit is the first porphyry-type copper deposit discovered with giant prospect in the Bangongco metallogenic belt. Geochemical data indicates that the ore-bearing Duobuza granodiorite porphyry is high-K calc-alkaline to shoshonitic and peraluminous composition. The ore-bearing granodiorite porphyry is enriched in large-ion lithophile elements(LILE) such as Rb, K, Th, La, Ce and Sr, and depleted in high-field-strength elements(HFSE) such as Nb, Ta, P, and Ti. The rare-earth element (REE) patterns show enrichment in light REEs relative to heavy REEs. The major, rare-earth, and trace elements of the ore-bearing granodiorite porphyry show characteristics of adakites, formed in an island arc setting. The laser ablation inductively coupled plasma-mass spectrometry (LA-ICP-MS) zircon U–Pb age of the ore-bearing granodiorite porphyry is 123.4±1.2 Ma (MSWD = 1.7), which also represents the age of the copper-mineralization. Together with the age data of the early Cretaceous magmatic rocks in the Bangongco–Nujiang suture zone and the middle-northern Gangdese, it indicates that there was bidirectional (northward and southward) subduction of the Bangongco–Nujiang ocean during 120 Ma, and the Duobuza deposit was related to this event.

**Keywords**: Granodiorite Porphyry, zircon LA-ICP-MS U–Pb age, Duobuza, tectonic setting, Tibet

## INTRODUCTION

The Duobuza porphyry copper deposit was the first to be discovered in the Bangongco metallogenic belt, located at the northern margin of the Bangongco–Nujiang suture zone separating the Qiangtang and Lhasa terranes, and represents a giant prospect (with inferred resources of 2.7 Mt Cu with an average grade of 0.94% and 13 t Au with an average grade of 0.21 g/t). Although the Duobuza deposit has been studied in terms of fluid-inclusion characteristics (She et al., 2006; Li et al., 2007; Li et al., 2011a), geochronology and geochemistry (Qu and Xin, 2006; Li et al., 2008; She et al., 2009; Li et al., 2011b), and hydrothermal alteration (Li et al., 2012), all these studies focused on the central and eastern ore-bearing rocks of the deposit and no investigation has focused on the western part of the Duobuza deposit because of limited exploration. Previous studies have shown that the ore bodies were mainly located in eastern and central granodiorite and sandstone, and there was no ore-bearing granodiorite porphyry in the western part. With further exploration, ore-bearing granodiorite porphyry was discovered in the western part. Geochemical characteristic, age of the rock, tectonic status and duration of deposit evolution are not clear. In this study, we present new work on geochemical properties (major and trace elements) of ore-bearing granodiorite porphyry in the western part of the Duobuza porphyry copper deposit. Also, we focus on the formation age using precise laser ablation inductively coupled plasma-mass spectrometry (LA-ICP-MS) zircon U–Pb geochronological dating. Finally, we discuss the duration of evolution of the deposit as well as implications on the tectonic setting of the Bangongco metallogenic belt.

0016-7622/2015-86-2-223/$ 1.00 © GEOL. SOC. INDIA

## GEOLOGICAL BACKGROUND

The Duobuza porphyry copper deposit is situated about 80 kms to the northwest of Gerze town, west Tibet, being structurally located on the northern side of the Bangongco–Nujiang suture zone and on the southern margin of the Qiangtang terrane (Fig. 1a). The rocks in the Duobuza deposit area belong to the lower Jurassic Quse Formation ($J_1q$), the lower Cretaceous Meiriqie Formation ($K_1m$), the Neogene Kangtuo Formation ($N_1k$), and the Quaternary system (Fig. 1b). The orebody is located in granodiorite porphyry and at the edge of propylitized sandstone of lower Jurassic Quse Formation.

The orebody has a width of about 100 to 400 m in the north–south direction and a length of about 1,400 m in the east–west direction, it extends vertically about 500 m from the outcrop, and dips toward 200° with a dip angle between 65° and 80°. The structures of the ore include primary disseminated veinlet and secondary brecciated and vein types. The ore minerals are mainly chalcopyrite, pyrite, magnetite, bornite, and molybdenite. There are three main alteration zones from the center of the rock body outward: a

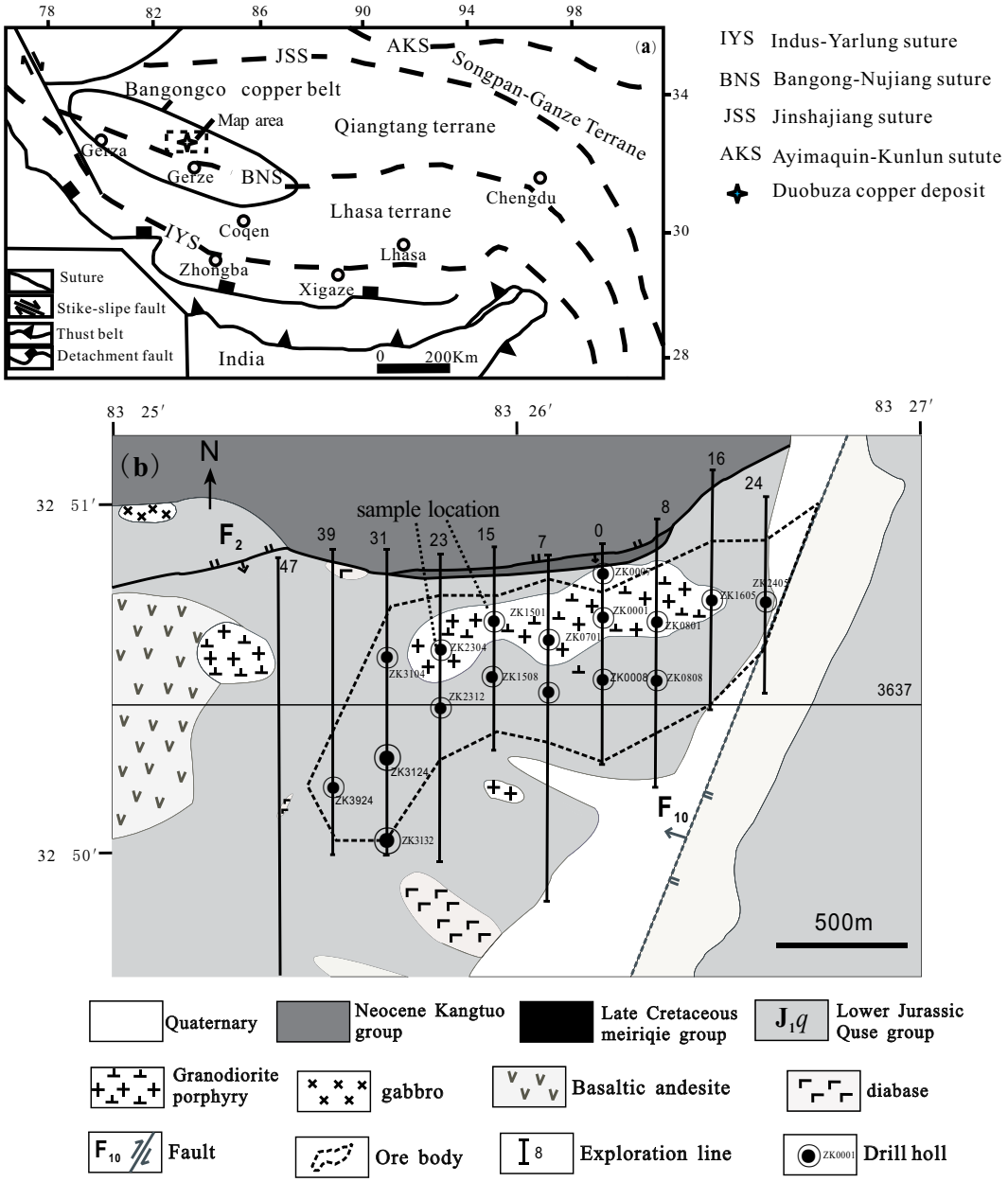


**Fig.1. (a)** Tectonic and location map (*after* Hou et al. 2004) **(b)** Generalized geological map of the Duobuza porphyry deposit in the Bangongco tectonic belt (*after* Li et al. 2011a).

potassic silicification zone, an argillization zone, and a limonitization zone–hornfels zone or propylitization zone. However, the phyllic alteration zone is not well developed, and sericite–quartz veinlets occur only locally.

## SAMPLING AND ANALYTICAL METHODS

All samples used in the present study were collected from two drill holes (Drillholes 2304 and 1501) and outcrops in exploration line Nos. 23 and 15 in the Duobuza deposit area, that is, from the west and at the margin of the ore body. Sample DBZ048, collected from Drillhole 2304, was used for zircon U–Pb dating. The depths of these two drill holes are, 610 and 520 m respectively, and both drill holes are almost entirely mineralized. Previous research mainly focused on the eastern and central parts of the deposit (exploration line Nos. 0, 8, and 16).

The ore-bearing granodiorite porphyry shows porphyritic texture and massive. The phenocrysts are quartz, plagioclase, K-feldspar, and biotite, with sizes ranging from 0.5 to 3.5 mm, and account for 25% to 40% by volume. The matrix components are quartz, plagioclase, biotite and as well as accessory minerals including tuff, zircon, rutile, magnetite, and pyrite, with sizes mainly ranging from 0.1 to 0.2 mm.

The ore-bearing granodiorite porphyry is more or less altered. Samples were taken from the least-altered granodiorite porphyry as far as possible. After the surface-weathered layer were removed, the samples were crushed roughly and then powdered manually in an agate mortar and washed with chemically pure ethyl alcohol and the treated samples were then used for analysis. The analysis of major elements and trace elements were done at the Analytical Center of Southwest Metallurgical Geology, Chengdu, China. The major elements were analyzed by a Rigaku RIX 2100 X-ray fluorescence (XRF) spectrometer using fused glass dicks, with an accuracy of better than 5%. The trace elements were analyzed by an ICP-MS (Agilent 7500a) after acid digestion of samples in a teflon bomb, and the accuracy was generally better than 10%.

Zircons were separated in the Geological Laboratory of Hebei Institute of Regional Geological Survey. And the LA-ICP-MS analysis of zircons were carried out at the State Key Laboratory of Continental Dynamics, Northwest University. Very transparent and well-crystallized zircon grains without fissures or inclusions were picked out from the separated zircons under a binocular microscope and then mounted in epoxy resin and polished until the grain interiors were exposed. Before analysis, the surface of zircon grain samples were cleaned using 3% diluted $HNO_3$ to remove any contaminant. Afterward, the internal structure were analyzed using cathode luminescence (CL) and *in situ* trace element analysis was conducted using a LA-ICP-MS. The zircon CL analysis was conducted on a Mono CL3+ system fitted to a field emission scanning electron microscope from FEI Company (USA). The ICP-MS used for zircon U–Pb dating was an Agilent 7500a with ShieldTorch, the latest-generation product from Agilient Company. The laser ablation system was a Geolas 200M produced by MicroLas Company (Germany), which was composed of a COMPex 102 excimer laser (whose working condition was ArF, operated at a wavelength of 193 nm, with a beam diameter of 32 ìm) from Lambda Physik Company (Germany) and an optical system from MicroLas Company. The detailed analysis method has been given by Yuan et al. (2008).

Before data analysis, synthetic silicate glass standard reference material NIST 610, developed by the National Institute of Standards and Technology (NIST), was used to optimize the instrument so that it reached its maximum sensitivity, minimum oxide yield ($ThO^+/Th^+ < 2\%$), and minimum background value. One Zircon 91500 and one NIST 610 were tested for every 5 sample points tested. Data processing was conducted using the GLITTER program (Version 4.0) and fractionation correction of isotopic ratios was done using Zircon 91500 as an external standard for the age calculation (Jackson et al., 2004). The concordia diagram for zircons was obtained with the ISOPLOT program (Version 3.0) (Ludwig, 2003). Details of the analytical procedures have been described by Yuan et al. (2004).

## ANALYTICAL RESULTS

### Zircon Cathodoluminescence (CL) Image and U–Pb Data

The zircon CL images of the granodiorite porphyry are shown in Fig. 2, and the geochronological results are given in Table 1. The zircons in the Duobuza granodiorite porphyry have high degree of euhedrism, showing euhedral to subhedral, with large grain size, ranging from 50 to 250 μm, indicating obvious magmatite crystal zoning. The zircon Th/U ratios range from 0.41 to 0.99 with an average of 0.62 and all are higher than 0.1, indicating that the zircons have a magmatic origin. Therefore, the crystallization age of the zircons can represent the rock-forming age of the granodiorite porphyry. The weighted mean age of 21 zircon grains is 123.4 ± 1.2 Ma (MSWD = 1.7) (Fig. 3), indicating that the ore-bearing granodiorite porphyry in the Duobuza porphyry copper deposit formed in the middle to early Cretaceous.

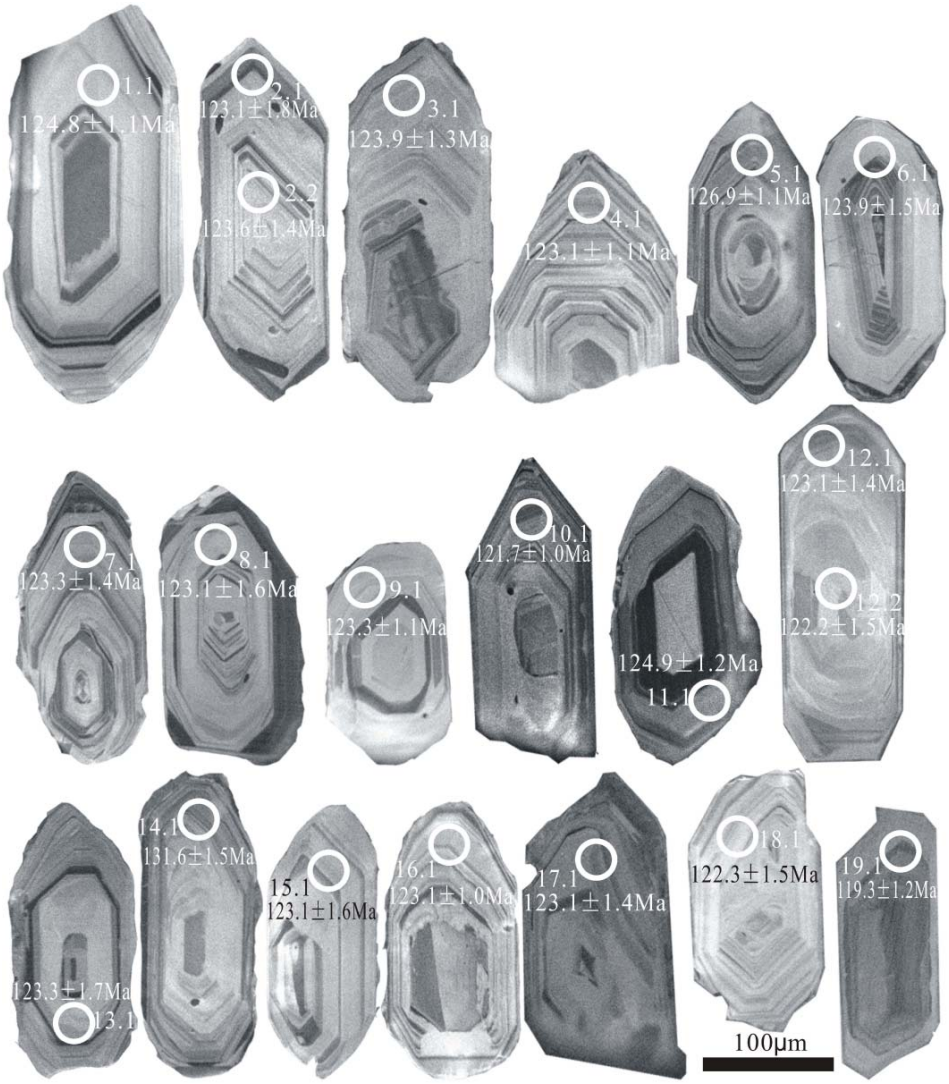


**Fig.2.** CL images for zircon from DBZ048.

**Rare-Earth Element Characteristics of the Zircons**

The rare-earth element (REE) results of the zircons are given in Table 2. After the analytical values were chondrite normalized (Sun and McDonough, 1989), the distribution diagrams (Fig. 4) were obtained. The diagrams indicate that all zircon cores have typical magmatic zircon REE distributions, that is, enrichment in heavy rare-earth elements (HREEs), depletion in light rare earth elements(LREE), and strong positive Ce anomalies,showing an REE mode with a leftward deviating distribution curve

**Major and Trace Element Characteristics**

The major and trace element analysis results are given in Table 3. In the ore-bearing granodiorite porphyry samples, $SiO_2$ content ranges from 62.14% to 68.49%, $Al_2O_3$ content ranges from 14.31% to 15.38%, MgO content ranges from 1.19% to 2.50%, CaO content ranges from 1.50% to 3.26%, $K_2O$ content ranges from 3.99% to 4.82%, and $Na_2O$ content ranges from 1.72% to 2.90% with $K_2O/Na_2O$ = 1.29–2.86. They are peraluminous, with A/CNK [molar ratios of $Al_2O_3$/($CaO + Na_2O + K_2O$)] = 1.07–1.58 (Fig. 5), and mainly lie within the high-K calc-alkalinc to shoshonitic field in the diagram of $K_2O$ vs $SiO_2$ (Fig. 6).

The REE distribution shows enrichment in (LREEs),and depletion in LREEs(Fig. 7), with moderate differentiation of LREE and HREEREE patterns. The total REE contents vary little, approximately from $37.26 \times 10^{-6}$ to $63.89 \times 10^{-6}$, showing few weak Ce anomalies (ΣCe = 0.76–0.93) but a positive Eu anomalies (ΣEu = 0.92–1.56). Positive Eu anomalies indicate that significant plagioclase crystal differentiation occurred in the original magma of the Duobuza granodiorite porphyry. The ore-bearing granodiorite porphyry exhibit similar primitive mantle-normalized patterns in the spidergrams(Fig. 8). They show

**Table 1.** Result of U-Pb zircon dating for the granodiorite porphyry(DBZ048) from Duobuza deposit.

| Spot | | | | Isotopic ratios | | | | | | | | | Age(Ma) | | | |
|---|---|---|---|---|---|---|---|---|---|---|---|---|---|---|---|---|
| | Th | U | Th/U | $^{238}U/^{232}Th$ | $^{207}Pb/^{206}Pb$ | 1σ | $^{207}Pb^*/^{235}U$ | 1σ | $^{206}Pb/^{238}U$ | 1σ | $^{207}Pb/^{206}Pb$ | 1σ | $^{208}Pb/^{232}Th$ | 1σ | $^{206}Pb/^{238}U$ | 1σ |
| 1.1 | 252 | 521 | 0.48 | 2.03 | 0.0698 | 0.0037 | 0.1859 | 0.0092 | 0.0195 | 0.0002 | 924 | 107 | 151 | 5 | 125 | 1 |
| 2.1 | 219 | 406 | 0.54 | 1.94 | 0.0789 | 0.0056 | 0.2105 | 0.0164 | 0.0193 | 0.0003 | 1170 | 142 | 196 | 37 | 123 | 2 |
| 2.2 | 187 | 367 | 0.51 | 1.90 | 0.0600 | 0.0036 | 0.1584 | 0.0095 | 0.0194 | 0.0002 | 606 | 125 | 126 | 5 | 124 | 1 |
| 3.1 | 172 | 310 | 0.55 | 1.77 | 0.0512 | 0.0044 | 0.1345 | 0.0112 | 0.0194 | 0.0002 | 250 | 200 | 125 | 5 | 124 | 1 |
| 4.1 | 509 | 699 | 0.73 | 1.36 | 0.0596 | 0.0025 | 0.1586 | 0.0069 | 0.0193 | 0.0002 | 591 | 93 | 99 | 3 | 123 | 1 |
| 5.1 | 635 | 987 | 0.64 | 1.58 | 0.0553 | 0.0025 | 0.1490 | 0.0062 | 0.0199 | 0.0002 | 433 | 98 | 107 | 3 | 127 | 1 |
| 6.1 | 536 | 992 | 0.54 | 1.84 | 0.0640 | 0.0023 | 0.1714 | 0.0067 | 0.0194 | 0.0002 | 740 | 74 | 130 | 4 | 124 | 1 |
| 7.1 | 488 | 771 | 0.63 | 1.57 | 0.0491 | 0.0035 | 0.1322 | 0.0092 | 0.0193 | 0.0002 | 150 | 159 | 106 | 5 | 123 | 1 |
| 8.1 | 189 | 312 | 0.61 | 1.61 | 0.0500 | 0.0055 | 0.1313 | 0.0145 | 0.0193 | 0.0003 | 195 | 237 | 129 | 7 | 123 | 2 |
| 9.1 | 388 | 579 | 0.67 | 1.47 | 0.0528 | 0.0026 | 0.1391 | 0.0067 | 0.0193 | 0.0002 | 317 | 111 | 121 | 3 | 123 | 1 |
| 10.1 | 362 | 626 | 0.58 | 1.68 | 0.0472 | 0.0027 | 0.1222 | 0.0068 | 0.0191 | 0.0002 | 58 | 130 | 113 | 3 | 122 | 1 |
| 11.1 | 733 | 1008 | 0.73 | 1.33 | 0.0550 | 0.0024 | 0.1474 | 0.0064 | 0.0196 | 0.0002 | 409 | 98 | 126 | 3 | 125 | 1 |
| 12.1 | 181 | 433 | 0.42 | 2.32 | 0.0535 | 0.0033 | 0.1402 | 0.0086 | 0.0193 | 0.0002 | 350 | 136 | 147 | 6 | 123 | 1 |
| 12.2 | 239 | 316 | 0.76 | 1.30 | 0.0620 | 0.0072 | 0.1434 | 0.0179 | 0.0191 | 0.0002 | 672 | 218 | 134 | 5 | 122 | 1 |
| 13.1 | 448 | 610 | 0.74 | 1.36 | 0.0659 | 0.0024 | 0.1751 | 0.0068 | 0.0193 | 0.0003 | 1200 | 78 | 149 | 4 | 123 | 2 |
| 14.1 | 312 | 582 | 0.54 | 1.83 | 0.1363 | 0.0073 | 0.4106 | 0.0246 | 0.0206 | 0.0002 | 2181 | 94 | 298 | 15 | 132 | 1 |
| 15.1 | 243 | 461 | 0.53 | 1.86 | 0.0506 | 0.0044 | 0.1323 | 0.0117 | 0.0193 | 0.0003 | 220 | 6 | 86 | 7 | 123 | 2 |
| 16.1 | 355 | 599 | 0.59 | 1.65 | 0.0590 | 0.0022 | 0.1559 | 0.0059 | 0.0193 | 0.0002 | 569 | 86 | 129 | 4 | 123 | 1 |
| 17.1 | 444 | 614 | 0.72 | 1.35 | 0.0477 | 0.0032 | 0.1255 | 0.0083 | 0.0193 | 0.0002 | 83 | 156 | 133 | 4 | 123 | 1 |
| 18.1 | 241 | 417 | 0.58 | 1.68 | 0.0638 | 0.0044 | 0.1670 | 0.0109 | 0.0191 | 0.0002 | 744 | 144 | 107 | 5 | 122 | 1 |
| 19.1 | 1982 | 1999 | 0.99 | 0.96 | 0.0515 | 0.0019 | 0.1332 | 0.0053 | 0.0187 | 0.0002 | 265 | 87 | 112 | 5 | 125 | 1 |

**Table 2.** REE content($10^{-6}$) of the zircons from the granodiorite porphyry(DBZ048)

| Spot | La | Ce | Pr | Nd | Sm | Eu | Gd | Tb | Dy | Ho | Er | Tm | Yb | Lu |
|---|---|---|---|---|---|---|---|---|---|---|---|---|---|---|
| 1.1 | 0.01 | 37.12 | 0.02 | 0.82 | 1.71 | 0.93 | 10.73 | 4.23 | 60.10 | 27.96 | 152.51 | 40.47 | 473.80 | 120.65 |
| 2.1 | 11.19 | 51.01 | 2.24 | 9.38 | 3.06 | 0.94 | 13.02 | 5.15 | 71.69 | 33.75 | 186.40 | 50.08 | 559.46 | 142.00 |
| 2.2 | 0.02 | 25.01 | 0.03 | 0.77 | 1.40 | 0.70 | 9.61 | 3.92 | 54.79 | 25.34 | 138.52 | 36.71 | 427.17 | 109.34 |
| 3.1 | 0.07 | 24.30 | 0.06 | 0.54 | 1.39 | 0.68 | 10.48 | 4.32 | 59.46 | 27.79 | 152.82 | 40.93 | 478.05 | 122.89 |
| 4.1 | 0.06 | 51.60 | 0.07 | 1.30 | 3.33 | 1.10 | 16.01 | 6.68 | 87.39 | 38.08 | 206.97 | 52.12 | 578.72 | 139.33 |
| 5.1 | 0.04 | 65.50 | 0.12 | 1.40 | 3.51 | 1.50 | 23.44 | 9.18 | 124.54 | 58.87 | 310.70 | 80.60 | 891.97 | 219.42 |
| 6.1 | 0.04 | 43.63 | 0.05 | 0.94 | 2.77 | 1.53 | 20.67 | 7.79 | 106.67 | 47.56 | 246.04 | 62.30 | 688.61 | 165.47 |
| 7.1 | 0.01 | 56.10 | 0.05 | 1.33 | 2.89 | 1.40 | 19.47 | 8.38 | 119.50 | 57.91 | 305.79 | 79.72 | 903.22 | 223.44 |
| 8.1 | 5.49 | 38.50 | 1.58 | 7.93 | 3.24 | 0.90 | 17.43 | 5.83 | 74.55 | 32.30 | 167.06 | 40.42 | 446.94 | 105.68 |
| 9.1 | 0.07 | 38.02 | 0.07 | 1.16 | 2.37 | 1.35 | 18.65 | 6.71 | 91.13 | 41.86 | 219.71 | 56.19 | 626.44 | 153.86 |
| 10.1 | 0.85 | 38.28 | 0.22 | 1.81 | 2.62 | 0.95 | 13.59 | 5.26 | 72.10 | 32.54 | 177.67 | 46.39 | 520.04 | 129.87 |
| 11.1 | 0.80 | 47.23 | 0.23 | 1.83 | 3.48 | 1.33 | 22.37 | 8.84 | 121.70 | 57.35 | 301.04 | 78.05 | 856.02 | 208.79 |
| 12.1 | 0.01 | 26.50 | 0.03 | 0.30 | 1.16 | 0.68 | 8.75 | 3.35 | 47.07 | 22.13 | 122.42 | 32.60 | 374.88 | 95.76 |
| 12.2 | 0.05 | 23.09 | 0.14 | 2.23 | 4.14 | 1.79 | 19.74 | 6.60 | 81.08 | 33.60 | 167.01 | 41.48 | 462.76 | 113.42 |
| 13.1 | 0.07 | 37.02 | 0.07 | 1.26 | 2.39 | 1.45 | 18.85 | 7.71 | 81.13 | 43.86 | 209.71 | 50.19 | 526.44 | 150.86 |
| 14.1 | 9.19 | 50.70 | 1.79 | 6.35 | 2.98 | 0.93 | 13.71 | 5.02 | 67.66 | 31.45 | 168.31 | 43.63 | 505.70 | 129.11 |
| 15.1 | 0.04 | 30.74 | 0.06 | 0.61 | 1.64 | 0.81 | 12.66 | 4.69 | 66.72 | 30.63 | 172.02 | 44.72 | 518.65 | 133.10 |
| 16.1 | 0.22 | 41.72 | 0.06 | 1.11 | 2.23 | 0.97 | 16.19 | 6.22 | 88.81 | 40.79 | 224.29 | 58.11 | 662.00 | 167.13 |
| 17.1 | 0.31 | 34.95 | 0.08 | 1.44 | 1.93 | 0.97 | 13.59 | 5.92 | 80.01 | 36.80 | 199.65 | 50.70 | 567.71 | 143.07 |
| 18.1 | 0.02 | 28.14 | 0.04 | 0.83 | 1.59 | 0.78 | 11.83 | 4.52 | 64.56 | 28.49 | 157.65 | 41.93 | 471.40 | 120.54 |
| 19.1 | 0.33 | 111.16 | 0.11 | 2.35 | 6.11 | 3.06 | 40.82 | 15.87 | 219.33 | 96.56 | 504.86 | 125.59 | 1390.46 | 340.30 |

strong enrichment in large-ion lithophile elements (LILE, e.g., Rb, K, Th, La, Ce, and Sr), and the depletion of high-field-strength elements (HFSE,e.g., Nb, Ta, P, and Ti), which is an essential characteristics of island arc.

## DISCUSSION

### Rock-forming and Ore-forming Ages

Sample DBZ048 for dating was collected from exploration line No. 23 (ZK2304) on the western margin of the Duobuza deposit, and the zircon U–Pb age obtained from the sample was 123.4 ± 1.2 Ma (MSWD = 1.7), so the ore-bearing granodiorite porphyry formed in the early Cretaceous. Previous samples for dating ore-bearing rock were basically taken from the eastern and central parts of the Duobuza deposit (exploration line No. 0 and outcrops). The ages obtained by previous researchers, ranged from 116.4Ma to 127.8 Ma (Table 4) for the Duobuza deposit, which is consistent with the result obtained from our study. The Re–Os model ages of molybdenite from the Duobuza deposit range from 117.6±1.3 to 118.5±1.4 Ma, and its isochron age is 118.0±1.5 Ma (She et al., 2009), slightly later than the rock-forming age of the ore-bearing porphyry, which also confirms the formation of Duobuza porphyry copper deposit in the early Cretaceous.

According to existing geochronological data for Duobuza porphyry deposit(Table 4), duration of magmatism can be defined at three stages: 116.4 Ma, 121.6-123.4 Ma

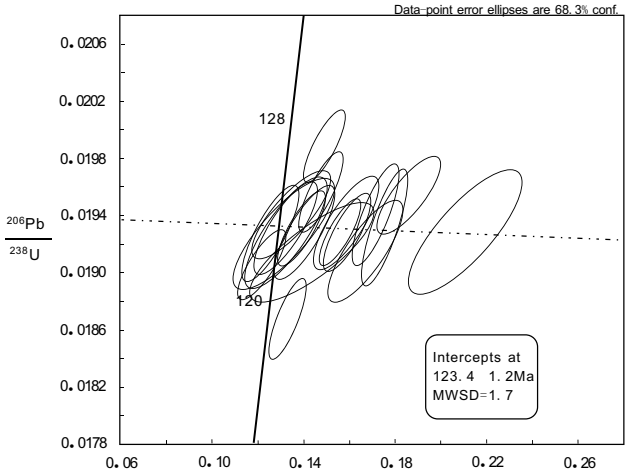


**Fig.3.** LA-ICP MS U–Pb Concordia diagrams for zircon from DBZ048.

and 127.8 Ma. Re–Os model ages of molybdenite ranged from 117.6 ± 1.3 to 118.5 ± 1.4 Ma, which presumably shows that 121.6-123.4 Ma is the most important diagenetic stage, mineralization mainly occurs in 118.0 ±1.5 Ma, formed in the early Cretaceous. The above mentioned analysis indicates that the eastern, central and west parts of the Duobuza ore-bearing granodiorite belong to the same ore-forming system under the same metallogenic setting, and its rock-forming and ore-forming processes are controlled by the same deep metallogenic dynamic process.

**Geochemistry of the Ore-bearing Granodiorite for Petrogenesis**

The ore-bearing granodiorite porphyry in the Duobuza deposit contains >56% $SiO_2$, > 15% (mean = 15.16%) $Al_2O_3$, < 3.0% MgO, low amounts of Y and Yb, and high amounts of Sr, high Sr/Y and La/Yb ratios; it is enriched in large-ion lithophile elements and depleted in HFSEs; and it is enriched in LREEs and depleted in HREEs, exhibiting the

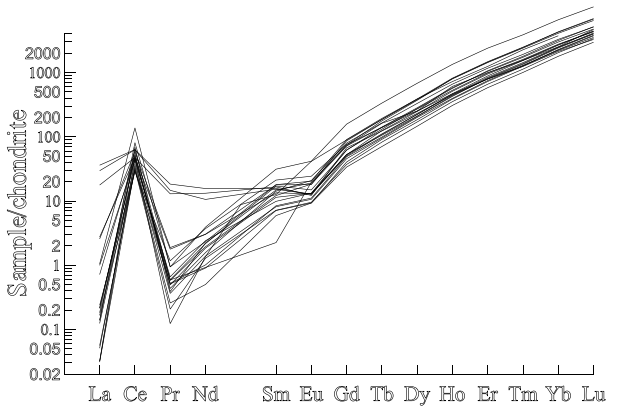


**Fig.4.** Chondrite normalized REE patterns of zircon for DBZ048 (*after* Sun and McDonough, 1989).

**Table 3.** Major and trace element analyses of the granodiorite porphyry.

| Sample | DBZ-035 | DBZ-039 | DBZ-046 | DBZ-048 | DBZ-052 | DBZ-057 | DBZ-062 |
|---|---|---|---|---|---|---|---|
| $SiO_2$ | 65.53 | 66.30 | 62.14 | 65.18 | 64.70 | 68.49 | 65.71 |
| $TiO_2$ | 0.35 | 0.33 | 0.58 | 0.35 | 0.36 | 0.27 | 0.41 |
| $Al_2O_3$ | 15.38 | 15.14 | 15.96 | 15.47 | 14.64 | 14.31 | 15.24 |
| TFeO | 4.08 | 3.58 | 6.85 | 4.38 | 5.69 | 3.13 | 4.92 |
| MnO | 0.06 | 0.04 | 0.11 | 0.07 | 0.05 | 0.05 | 0.09 |
| MgO | 1.44 | 1.50 | 2.50 | 1.42 | 1.45 | 1.19 | 1.67 |
| CaO | 3.26 | 2.65 | 1.50 | 3.01 | 2.40 | 2.20 | 2.48 |
| $Na_2O$ | 2.46 | 2.78 | 1.92 | 2.90 | 1.72 | 2.53 | 2.06 |
| $K_2O$ | 3.99 | 4.60 | 3.92 | 3.75 | 4.82 | 4.79 | 4.31 |
| $P_2O_5$ | 0.14 | 0.10 | 0.16 | 0.13 | 0.11 | 0.07 | 0.11 |
| LOI | 3.38 | 3.10 | 4.51 | 2.98 | 3.86 | 3.13 | 4.20 |
| **Total** | **100.07** | **100.13** | **100.15** | **99.64** | **99.81** | **100.16** | **101.20** |
| A/CNK | 1.07 | 1.054 | 1.57 | 1.08 | 1.18 | 1.07 | 1.21 |
| Cu | 872 | 2200 | 8130 | 498 | 3160 | 3200 | 3340 |
| Pb | 17.1 | 20.3 | 24.9 | 24.6 | 15.0 | 24.2 | 22.7 |
| Cr | 11.9 | 10.4 | 23.8 | 13.8 | 13.8 | 16.0 | 14.7 |
| Ni | 3.12 | 5.36 | 34.3 | 4.04 | 3.17 | 8.77 | 9.08 |
| Co | 15.7 | 17.9 | 19.8 | 10.6 | 14.2 | 13.5 | 17.0 |
| Li | 27.6 | 23.2 | 24.0 | 19.5 | 17.0 | 20.2 | 20.0 |
| Rb | 123 | 134 | 155 | 128 | 176 | 122 | 147 |
| Cs | 7.08 | 6.81 | 6.77 | 6.26 | 6.10 | 5.25 | 7.37 |
| Mo | 13.9 | 2.76 | 13.6 | 4.96 | 10.5 | 29.4 | 29.6 |
| Sr | 386 | 433 | 241 | 439 | 303 | 344 | 331 |
| Ba | 521 | 574 | 357 | 495 | 786 | 534 | 560 |
| V | 57.7 | 46.2 | 101 | 55.6 | 64.7 | 60.2 | 71.8 |
| Sc | 8.36 | 7.63 | 11.2 | 7.30 | 7.08 | 6.27 | 7.65 |
| Nb | 6.2 | 5.93 | 7.88 | 6.1 | 6.45 | 5.24 | 6.59 |
| Ta | 0.53 | 0.51 | 0.65 | 0.5 | 0.57 | 0.49 | 0.58 |
| Zr | 83.5 | 77.1 | 93.1 | 85.5 | 75.7 | 79.6 | 78 |
| Hf | 2.86 | 3.23 | 5.75 | 3.12 | 3.56 | 3.5 | 3.72 |
| Ag | 0.40 | 0.41 | 1.54 | 0.32 | 1.12 | 0.69 | 0.78 |
| Au | 23.2 | 46.3 | 372 | 15.5 | 22.6 | 87.1 | 126 |
| U | 1.33 | 1.22 | 1.11 | 1.3 | 2.51 | 1.61 | 1.94 |
| Th | 8.64 | 11.9 | 8.82 | 8.54 | 11.5 | 9.28 | 10.9 |
| Y | 10.2 | 9.15 | 14.2 | 11.4 | 7.63 | 7.40 | 10.1 |
| La | 10 | 12.8 | 15.6 | 11.2 | 10.5 | 11.5 | 12.9 |
| Ce | 14.5 | 18.4 | 23.4 | 20.2 | 13.8 | 17.1 | 19.3 |
| Pr | 1.81 | 2.02 | 2.69 | 2.18 | 1.48 | 1.84 | 2.09 |
| Nd | 7.49 | 7.99 | 10.7 | 8.94 | 5.66 | 6.66 | 8.1 |
| Sm | 1.56 | 1.49 | 2.29 | 1.76 | 1.17 | 1.3 | 1.62 |
| Eu | 0.56 | 0.56 | 0.66 | 0.6 | 0.54 | 0.55 | 0.64 |
| Gd | 1.27 | 1.20 | 1.99 | 1.52 | 0.89 | 0.94 | 1.31 |
| Tb | 0.24 | 0.22 | 0.37 | 0.28 | 0.18 | 0.18 | 0.24 |
| Dy | 1.58 | 1.32 | 2.35 | 1.71 | 1.11 | 1.09 | 1.57 |
| Ho | 0.35 | 0.31 | 0.51 | 0.38 | 0.26 | 0.25 | 0.36 |
| Er | 1.00 | 0.85 | 1.50 | 1.11 | 0.74 | 0.72 | 1.09 |
| Tm | 0.14 | 0.12 | 0.21 | 0.16 | 0.11 | 0.095 | 0.16 |
| Yb | 0.96 | 0.80 | 1.42 | 1.02 | 0.71 | 0.71 | 1.12 |
| Lu | 0.15 | 0.13 | 0.21 | 0.17 | 0.12 | 0.11 | 0.19 |

characteristics of adakites (Defant and Drummond, 1990; Martin, 1999; Castillo, 2006). In the Sr/Y–Y diagram (Fig. 9), all the samples also plot within the area of adakites,too. The ore-bearing granodiorite porphyry from the eastrern and central of the deposit have the geochemical characteristics of high-K calc-alkalinc to shoshonitic, enrichment of light REEs, LILEs and depletion of HFSE as well as aking to adakites (Qu et al.,2006; Li et al., 2008; She et al., 2009), similar to western part.

The term adakite was originally proposed to define silica-rich, high Sr/Y and La/Yb volcanic and plutonic rocks derived from melting of the basaltic portion of oceanic crust

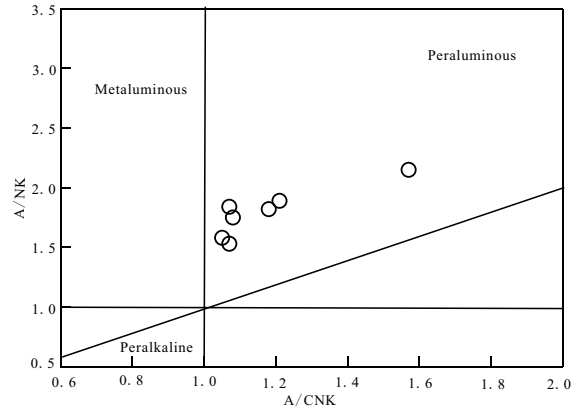


**Fig.5.** A/NK vs A/CNK plot for Duobuza granodiorite porphyry (*after* Shand, 1947).

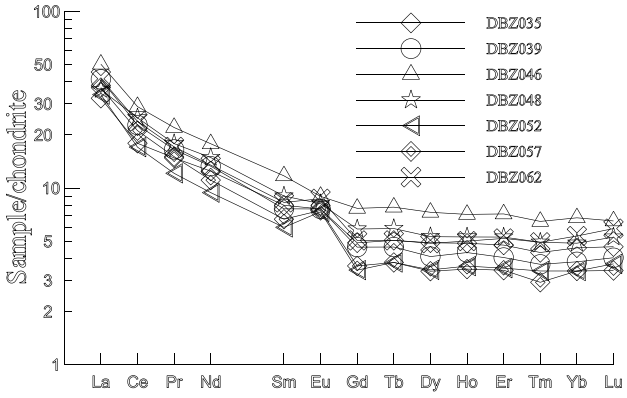


**Fig.7.** Chondrite normalized REE patterns for Duobuza granodiorite porphyry(*after* Sun and McDonough, 1989).

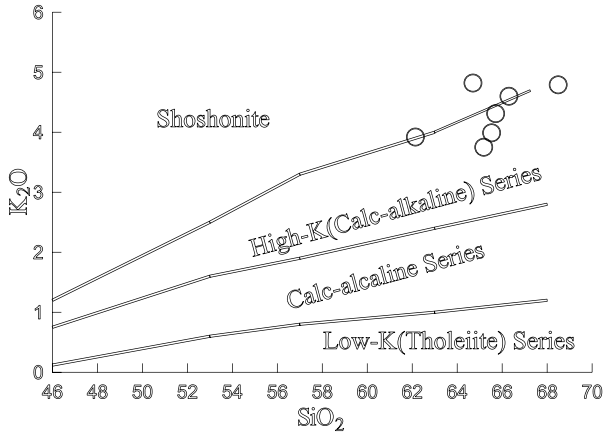


**Fig 6.** $K_2O$ vs $SiO_2$ plot for Duobuza granodiorite porphyry (*after* Rickwood, 1989).

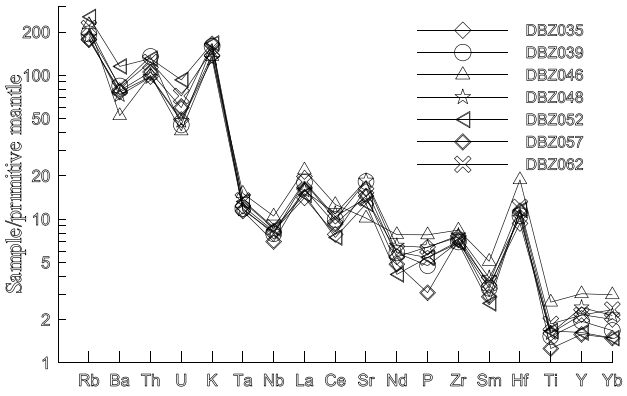


**Fig .8.** Primordial mantle normalized trace element patterns for Duobuza granodiorite porphyry(*after* Sun and McDonough, 1989)

subducted beneath volcanic arcs. It was also initially believed that adakite only occurs in convergent margins where young and hot oceanic slabs are being subducted, but later studies have proposed that it also occurs in other arc settings (Defant and Drummond, 1990; Martin, 1999; Defant et al., 2002; Castillo, 2006). It is shown that adakite has a close relationship with Cu, Au mineralization suggesting that the ore-forming material came from subducting plate (Defant and Drummond, 1990; Zhang et al., 1997; Li et al., 2008).

Enrichment in LREE and LILEs, depletions in HFSEs (Nb, Ta and Ti) demonstrate that the ore-bearing granodiorite porphyry have typical magmatic characteristics of subduction-related island-arc magma (Wilson, 1989). It is also opined that crustal sediments also contributed to the formation of island-arc magmatic rocks (Ben et al., 1989; McCulloch and Gamble, 1991; Hawkesworth, et al., 1993). The ore-bearing granodiorite porphyry in Duobuza deposit have a high $^{87}Sr/^{86}Sr$ ratios and a low $^{143}Nd/^{144}Nd$ ratios (Li et al., 2008), which suggest addition of sediment in the process of formation of adakites (Defant et al., 2002; Martin et al., 2005). Major, trace element geochemistry and Sr-Nd isotopes characteristics also suggest that the adakitic ore-bearing granodiorite porphyry in the Duobuza deposit

**Table 4.** Results of the ages for the Duobuza granodiorite porphyry

| Number | Sample | Analyzed rock | Method | age/Ma | ±σ | SMWD | Data sources |
|---|---|---|---|---|---|---|---|
| 1 | DBZ048 | Granodiorite porphyry | LA-ICPMS U-Pb | 123.4 | 1.2 | 1.7 | Present study |
| 2 | DBZJ2-1 | Ggranodiorite porphyry | SHRIMP U-Pb | 121.6 | 1.9 | 2.1 | Li et al., (2008) |
| 3 | ZK2-13 | Granodiorite porphyry | LA-ICPMS U-Pb | 127.8 | 2.6 | 1.18 | Qu and Xin, (2006) |
| 4 | DBZTC-6 | Granodiorite porphyry | LA-ICPMS U-Pb | 116.4 | 2.5 | 1.1 | Li et al, (2011b) |

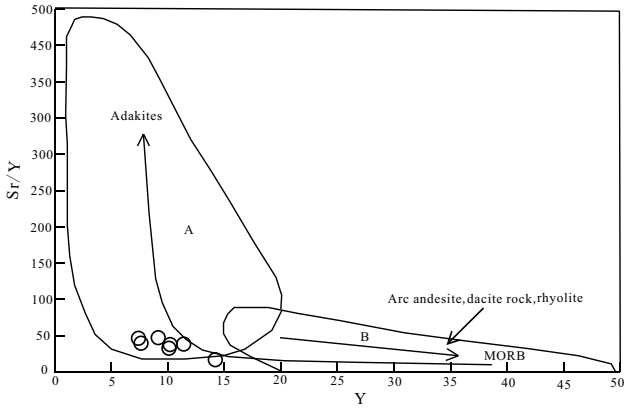


**Fig.9.** Y-Sr vs Y plot for Duobuza granodiorite porphyry(*after* Defant and Drummond, 1990)

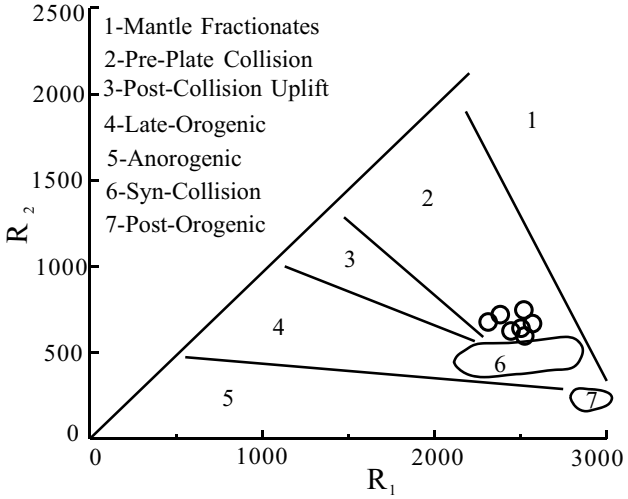


**Fig.10.** $R_2$ vs $R_1$ plots for Duobuza granodiorite porphyry (*after* Batchelor and Bowden,1985)

might have been directly derived from partial melting of subducting oceanic crust, with the addition of sediments during subduction.

**Implications on the Tectonic Setting**

In the $R_1$–$R_2$ diagram [where $R_1$ = 4Si-11(Na + K) - 2(Fe + Ti) and $R_2$ = 6Ca + 2Mg +Al] reflecting the tectonic evolution stages of the orogenic belt (Batchelor and Bowden, 1985), all the samples fall within the pre-plate-collision area, indicating an island arc subduction setting (Fig. 10). In addition, the spatial association of high-Nb basalt with "adakitic meta-somatic volcanic series"(Li et al., 2008), indicate Duobuza deposit form in the typical island arc subduction setting.

The opening and closure times of the Bangongco–Nujiang oceanic basin have been of considerable debate. Huang and Chen (1993) and Kapp et al. (2003) thought that the Bangongco–Nujiang Oceanic basin opened in the Triassic, expanded to form a deep oceanic basin in the early Jurassic, subducted northward under the Qiangtang block in the late Jurassic, and closed during the end of the late Jurassic and the beginning of the Cretaceous. It is worth noting that the subduction polarity of the Bangongco–Nujiang Neo-Tethys Ocean has been under considerable debate, with northward subduction during the late Triassic–early Cretaceous (Murphy et al., 1997; Kapp et al., 2003; Ding et al., 2003; Zhang et al., 2004; Li et al., 2008) to southward subduction during the late Jurassic–early Cretaceous (Pan et al., 1997; Mo et al., 2005; Zhu et al., 2009) and to bidirectional subduction during the late Jurassic–early Cretaceous (Pan et al., 2004; Qin et al., 2006; Du et al., 2011). Qin et al. (2006) primarily believed based on research work, that the Bangongco–Nujiang Neo-Tethys Ocean experienced at least three subduction stages, i.e., northward subduction during the late Triassic–early Cretaceous, bidirectional (northward and southward) subduction during the early stage of the middle and late Jurassic–early Cretaceous, and collision during the middle Cretaceous. Pan et al. (2004) thought that the Bangongco–Nujiang suture zone was in a multi-island arc basin series within ocean–continent transition phase during the late Jurassic to the early stage of the early Cretaceous, at which time the predominant feature was generation of large-scale island-arc-type volcanic magmatism and bidirectional subduction. Zhu et al. (2006) considered that the late Jurassic–early Cretaceous volcanic rocks on the middle-northern Gangdese (belt) were related to southward subduction of the Bangongco–Nujiang Neo-Tethys oceanic crust. The early Cretaceous granodiorite porphyry (124.4 ± 1.9 Ma) and allgovite (117.1 ± 1.0 Ma) in the Dongzhongla area (eastern section of the middle Gangdese) in the eastern Gangdese were regarded as the result of bidirectional subduction, i.e., southward subduction of the Bangongco–Nujiang suture zone and northward subduction of the Neo-Tethys ocean (Fei et al., 2010a,b). The central Lhasa sub-terrane (middle Gangdese) experienced a long period of magmatism in the early Cretaceous (143–102 Ma) with strong input of mantle-derived materials at 110 Ma, which can be explained by the break-up of the southward subducting Bangong–Nujiang ocean seafloor during the Lhasa–Qiangtang collision (Zhu, et al., 2009). The rock-forming age of the ore-bearing granodiorite porphyry in Duobuza located to the north of the Bangongco–Nujiang suture zone in Tibet is 123.4 ±1.2 Ma (MSWD = 1.7), which, together with the age data of the early Cretaceous magmatic rocks in the Bangongco–Nujiang suture zone and the middle-northern Gangdese, indicates that there was bidirectional (northward and southward) subduction of the Bangongco–

Nujiang ocean during 120 Ma. The Duobuza porphyry copper deposit was related to this bidirectional (northward and southward) subduction of the Bangongco–Nujiang Neo-Tethys ocean.

## CONCLUSIONS

Based on the geochronological and geochemical studies the following conclusions are drawn:

1 The Duobuza ore-bearing granodiorite porphyry are enriched in LREEs and LILEs such as Rb, K, Th, La, Ce, and Sr, and depleted in HREEs and HFSEs, such as, Nb, Ta, P, and Ti. Further zircon U–Pb dating yields a crystallization age of 123.4 ± 1.2 Ma.

2 The Duobuza ore-bearing granodiorite porphyry have geochemical affinity to adakites. These adakitic rocks were derived from partial melting of subducting oceanic crust, with an island arc subduction setting.

3 The Duobuza deposit was related to bidirectional subduction of the Bangongco–Nujiang ocean in the early Cretaceous.

*Acknowledgments:* This study was funded by the Public Sector Research and Development Project of the Ministry of Land and Resources (201011013), China Geological Survey Bureau (1212011121271), the National Key Cultivating Disciplines Mineralogy, Petrology, and Mineral Deposits (SZD0407), Opening Foundation of Key Laboratory of Tectonic Controls on Mineralization and Hydrocarbon Accumulation,Ministry of Land and Resources (gzck2013006) and Tectonic metallogeny theory development and practice team fund of Sichuan Province(13TD0008). The authors express their appreciation for beneficial direction from Chao-qiang Liu, Yan-bo Li, and An-hui Fan from Geological Team No. 5 of the Tibet Bureau of Geology and Exploration for their assistance in the field investigation as well as constructive comments from anonymous reviewers and careful editorial handling.

## References

Batchelor, R.B. and Bowden, P. (1985) Petrogenetic interpretation of granitoid rock series using multicationic parameters. Chem. Geol, v.48, pp.43-55.

Ben, O.D., White, W.M. and Patchett, J. (1989) Geochemistry of marine sediments, island arc magma genesis, and crust-mantle recycling. Earth Planet. Sci. Lett, v.94, pp.1-21.

Castillo, P.R. (2006) An overview of adakite petrogenesis. Chinese Sci. Bull., v. 51, pp. 257-268.

Defant, M.J. and Drummond, M.S. (1990) Derivation of some modern arc magmas by melting of young subducted lithosphere. Nature, v.347, pp.662-665.

Defant, M.J., Xu, J.F., Kepezhinskas, P., Wang, Q., Zhang, Q. and Xiao, L.(2002) Adakites: some variations on a theme. Acta. Petrol. Sin, v.18, pp.129-142.

Ding, L., Kapp, P., Yin, A., Deng, W.M. and Zhong, D.L. (2003) Early Tertiary volcanism in the Qiangtang terrane of central Tibet: evidence for a transition from oceanic to continental subduction. Jour. Petrol., v.44, pp.1833-1865.

Du, D.D., Qu, X.M., Wang, G.H., Xin, H.B. and Liu, Z.B. (2011) Bidirectional subduction of the Middle Tethys oceanic basin in the west segment of Bangongco-Nujiang suture£¬Tibet: Evidence from zircon U-Pb LA-ICP MS dating and petrogeochemistry of arc granites. Acta. Petrol. Sin., v.27, pp.1993-2002.

Fei, G.C., Wen, C.Q., Wang, C.S., Zhou, X., Wu, P.Y., Wen, Q. and Zhou, Y.(2010a) Zircon SHRIMP U-Pb age of porphyry granite in Dongzhongla lead-zinic deposit, Mozhugongka County, Tibet. Geol. China, v.37, pp.470-476.

Fei, G.C., Wen, C.Q., Wang, C.S., Wu, P.Y., Wen, Q. and Zhou, X. (2010b) Zircon SHRIMP U-Pb age of allgovite in Dongzhongla, east gangdise, and it's geological significance. Geol. Bull. China, v.29, pp.1138-1142.

Grifin, W.L., Wang, X., Jackson, S.E., Pearson, N.J., O'Reilly, S.Y., Xu, X. and Zhou, X.(2002)Zircon chemistry and magma mixing, SE China: in-situ analysis of Hf isotopes.Tonglu and Pingtan igneous complexes. Lithos, v.61, pp.237-269.

Hou, Z.Q., Gao, Y.F., Qu, X.M., Rui, Z.Y. and Mo, X.X. (2004) Origin of adakitic intrusives generated during mid-Miocene East-west extension in southern Tibet. Earth Planet. Sci. Lett., v.220, pp.139-155.

Hawkesworth, C.J.,Gallagher, K., Hergt, J.M. and McDermott, F. (1993) Mantle and slab contributions in arc magmas. Ann. Rev. Earth Planet. Sci., v.21, pp.175-204.

Huang, J.Q and Chen, B.W. (1987) Geological evolution of Tethys sea around China and its adjacent areas. Beijing Geological Publishing House, pp.1-78.

Kapp, P., Murphy, M.A., Yin, A., Harrison, M.T., Ding, L. and Guo, J.H. (2003) Mesozoic and Cenozoic tectonic evolution of the Shiquanhe area of western Tibet. Tectonics, v.22, pp.10-29.

Li, G.M., Li, J.X., Qin, K.Z., Duo, J., Zhang, T. P., Xiao B. and Zhao, J.X. (2012) Geology and Hydrothermal Alteration of the Duobuza Gold-Rich Porphyry Copper District in the Bangongco Metallogenetic Belt, Northwestern Tibet. Resour. Geol., v.62, pp. 99-118.

Li, G.M., Li, J.X., Qin, K.Z., Duo, J., Zhang, T.P. and Xiao, B.(2007) High temperature, salinity and strong oxidation ore-forming fluid at Duobuza gold-rich porphyry copper in the Bangongco tectonic belt, Tibet: evidence from fluid inclusions study. Acta. Petrol. Sin., v.23, pp.935-52.

Li, J.X., Li, G.M., Qin, K.Z. and Xiao, B. (2011a) High temperature primarymagmatic fluid directly exsolved from magma at Duobuza gold-rich porphyry copper deposit, Northern Tibet. Geofluids, v.11, pp.134-143.

Li, J.X., Li, G.M., Qin, K.Z. and Xiao, B. (2008) Geochemistry of porphyries and volcanic rocks and ore-forming geochronology of Duobuza gold-rich porphyry copper deposit in Bangongco belt, Tibet: Constraints on metallogenetic tectonic settings. Acta. Petrol. Sin.,v.24, pp.531-543.

Li, J.X., Li, G.M., Qin, K.Z. and Xiao, B., Zhao, J. X. and Chen, L. (2011b) Magma-hydrothermal evolution of the Cretaceous Duolong gold-rich porphyry copper deposit in the Bangongco metallogenetic belt, Tibet: evidence from U-Pb and $^{40}Ar/^{39}Ar$ geochronology. Jour. Asian Earth Sci., v.41, pp.525-536.

Li, J.X., Li,G.M., Qin, K. Z.,Xiao, B., Chen, L. and Zhao, J. X.(2012) Mineralogy andmineral chemistry of the Cretaceous Duolong gold-rich porphyry copper deposit in the Bangongco arc,Northern Tibet. Resource Geol., v.62, pp.19-41.

Li, Y.B., Duo, J., Zhong, W.T., Li, Y.C., Qiangba, W.D., Chen, H.Q., Liu, H.F., Zhang, J.S., Zhang, T.P., Xu, Z.Z., Fan, A.H. and Suo Lang, W.Q. (2012) An exploration model of the Duobuza porphyry copper deposit in Gerze Couty, northern Tibet. Geol. Explor., v.48, pp.274-287.

Ludwig, K.R.(2003) Isoplot 3.0-A geochronological toolkit for Microsoft Excel[M]. Berkeley Geochronology Center, pp.1-70.

Martin, H. (1999) The adakitic magmas: modern analogues of Archaean granitoids. Lithos, v.46, pp.411-429.

Martin, H., Smithies, R.H.,Rapp,R.,Moyen, J.F. and Champion, D.(2005) An overview of adakite, tonalite–trondhjemite–granodiorite (TTG), and sanukitoid: relationships and some implications for crustal evolution. Lithos, v.79, pp.1-24.

McCulloch, M.T. and Gamble, J.A. (1991) Geochemical and geodynamical constraints on subduction zone magmatism. Earth Planet. Sci. Lett, v.102, pp.358-374.

Mo, X.X., Dong, G.C., Zhao, Z.D., Zhou, S., Wang, L.L., Qiu, R.Z. and Zhang, F.Q. (2005) Spatial and temporal distribution and characteristics of granitoids in the Gangdese, Tibet and implication for crustal growth and evolution. Geol. Jour. China Universities, v.11, pp.281-290.

Murphy, M.A., Harrison, T.M., Durr, S.B., Chen, Z., Ryerson, F.J., Kidd, W.S.F., Wang, X. and Zhou, X. (1997) Significant crustal shortening in south central Tibet prior to the Indo-Asian collision. Geology, v.25, pp.719-722.

Pan, G.T., Wang, L.Q. and Zhu, D.C.(2004) Thoughts on some important scientific problems in regional geological survey of the Qinghai-Tibet Plateau. Geol. Bull. China, v.23, pp.12-19.

Pan, G.T., Chen, Z.L., Li, X.Z., Yang, Y.J., Xu, X.S., Xu, Q., Jiang, X.S., Wu, Y.L., Luo, J.N., Zhu, T.X. and Peng, Y.M. (1997) Geological–Tectonic Evolution in the Eastern Tethys. Geological Publishing House, pp.1-218.

Peccerillo, A. and Taylor, S.R. (1976) Geochemistry of Eocene calc –alkaline volcanic rocks from the Kastamonu area, Northern Turkey. Contrib. Mineral. Petrol., v.1, pp.63-81.

Qu, X.M. and Xin, H.B. (2006) Ages and tectonic environment of the Bangong Co porphyry copper belt in western Tibet, China. Geol. Bull. China, v.25, pp.792-799.

Rickwood, P. C. (1989) Boundary lines within petrologic diagrams which use oxides of major and minor elements. Lithos, v.22, pp.247-263.

Shand, S.J. (1947) Eruptive rocks: their genesis, composition, classification, and their relation to ore-deposits, with a chapter on meteorites, 3rd edition. John Wiley, New York, 488p.

She, H.Q., Li, J.W., Ma, D.F., Li, G.M., Zhang, D.Q., Feng, C.Y., Qu, W.J. and Pan, G. T.(2009) Molybdenite Re-Os and SHRIMP zircon U-Pb dating of Duobuza porphyry copper deposit in Tibet and its geological implications. Miner. Deposit, v.28,pp.737-746.

Simon, E.J., Norman, J.P. and William, L.G.(2004) The application of laser ablation-inductively coupled plasma-mass spectrometry to in-situ U-Pb zircon geochronolgy. Chem. Geol, v.211, pp.47-69.

Sun, S.S. and McDonough, W.F. (1989) Chemical and isotopic systematics of oceanic basalts: implications for mantle composition and processes. *In:* M.J. Norry and A.D. Saunders (Eds.), Magmatism in the Ocean Basins. Geological Society Special Publication, London, pp.313-345.

Wilson, M. (1989) Igneous Petrogenesis: a global tectonic approach. Uniwin Hyman, London.

Yuan, H.L., Gao, S., Dai, M.N., Zong, C.L., Günther, D., Fontaine, G.H., Liu, X.M. and Diwu, C.R. (2008) Simultaneous determinations of U–Pb age, Hf isotopes and trace element compositions of zircon by excimer laser ablation quadrupole and multiple collector ICP-MS. Chem. Geol, v.247, pp.100-117.

Yuan, H.L., Gao, S., Liu, X.M., Li, H.M., Gunther, D. and Wu, F.Y.(2004) Accurate U-Pb age and trace element determinations of zircon by laser ablation-inductively coupled plasma mass spectrometry. Geostandards Newsletter, v.28, pp.353-370.

Zhang, K.J., Xia, B.D., Wang, G.M., Li, Y.T. and Ye, H.F. (2004) Early Cretaceous stratigraphy, depositional environments, sandstone provenance, and tectonic setting of central Tibet, western China. GSA Bull., v.116, pp.1202-1222.

Zhang, Q., Qin, K.Z., Wang, Y.L., Zhang, F.Q., Liu, H.T. and Wang, Y.(2004) Study on adakite broadened to challenge the Cu and Au exploration in China. Acta. Petrol. Sin., v.20, pp.195-204.

Zhu, D.C., Pan, G.T., Mo, X.X., Wang, L.Q., Liao, Z.L., Zhao, Z.D., Dong, G.C. and Zhou, C.Y.(2006) Late Jurassic–Early Cretaceous geodynamic setting in middle–northern Gangdese: new insights from volcanic rocks. Acta. Petrol. Sin., v.22,pp.534-546.

Zhu, D.C., Mo, X.X., Niu, Y.L., Zhao, Z.D., Wang, L.Q., Liu, Y.S. and Wu, F.Y. (2009) Geochemical investigation of Early Cretaceous igneous rocks along an east–west traverse throughout the central Lhasa Terrane, Tibet. Chem. Geol., v.268, pp.298-312.

*(Received: 17 December 2012; Revised form accepted: 5 May 2014)*